Dark energy at cosmological and astrophysical scales: theoretical models and observational tests

Bohdan Novosyadlyj[1·2]

1. Astronomical Observatory of Ivan Franko National University of Lviv, Kyryla i Methodia str., 8, Lviv, 79005, Ukraine,
2. International Center of Future Science of Jilin University, Qianjin Street 2699, Changchun, 130012, P.R.China

The properties and observational manifestations of dynamical dark energy at cosmological and astrophysical scales will be discussed. We will consider the dynamical dark energy in the form of the quintessential and phantom scalar fields with different values of equation of state parameters and effective sound speed. The evolution of the dynamical dark energy and its impact on the dynamics of expansion of the Universe, halos and voids, its behavior in the static world of galaxies, in the vicinities of stars and black holes will be analyzed. The current state and possible tests designed for establishing of the nature of dark energy will be highlighted in the lecture.

1 Introduction

Extragalactic and cosmological observational data collected up to now and interpreted in the framework of current physical theories certify that about 70% of the energy-mass content of our world is the dark energy which fills the Universe almost uniformly and accelerates its expansion. Its physical nature is still unknown because of its "darkness" and exclusively cosmological scale "fingerprints." The explanation of the nature of this mysterious component becomes extremely important for elaboration of the physics of galaxies and clusters, cosmology, and particle physics beyond the Standard Model. Among several hypotheses discussed in the literature about the nature of dark energy, the hypothesis that it is a scalar field with a violated weak or null energy condition seems the most promising in terms of the possibility to be tested by comparison of theoretical predictions with observational data. The scalar field can be quintessential dark energy, phantom or changing type from one to another (quintom) at different moments of time, or be vacuumlike (or Λ-type) dark energy. Here we will analyse the behavior, properties and possible observational manifestations of dynamical dark energy at cosmological and astrophysical scales.

2 Scalar field as dark energy

Cosmologists have enough observational evidence that our Universe is expanding with positive acceleration, instead of deceleration expected for a world filled with ordinary matter and described in the framework of general relativity. The physical essence which causes such unusual dynamics of whole world was called "dark energy" (Huterer & Turner, 1999). Since the dozens of thousands papers are devoted to the analysis of different models of dark energy (see, for example, books and few review articles Ellis et al., 2008; Amendola & Tsujikawa, 2010; Wolschin,

2010; Ruiz-Lapuente, 2010; Novosyadlyj et al., 2015). One of the most developed models in the terms of comparing of numerical predictions with observational data and determination of the parameters and their confidence intervals is a scalar field that fills the Universe almost homogeneously and slowly rolls down to the minimum of its own potential in the case of a quintessential scalar field or slowly rolls up to the maximum in the case of a phantom one. Here we try to elucidate the main properties and manifestations of scalar field dark energy in the cosmological background with Friedmann-Robertson-Walker metric, in the forming halos and voids, in the static world with Minkowski metric and in the vicinity of compact spherical bodies with Schwarzschild metric. There are many possible realizations of such fields, that is why the additional observational or experimental tests, which could help to constrain the number of candidates at least in the class of scalar field models of dark energy are needed.

Scalar field dark energy can be set by Lagrangian $\mathcal{L}(X,U)$ with a kinetic term $X \equiv \dot{\varphi}^2/2$ and a given potential $U(\varphi)$ or by energy-momentum tensor $T_{ij}(\rho_{\rm de}, p_{\rm de})$ in the phenomenological approach. In the last case as usual the dark energy is assumed to be the perfect fluid described by a smallest number of parameters: the density in units of critical one at current epoch $\Omega_{\rm de} \equiv \rho^0_{\rm de}/\rho^0_{\rm cr}$, the equation of state parameter $w_{\rm de} \equiv p_{\rm de}/\rho_{\rm de} < -1/3$ and the square of effective sound speed $c^2_{\rm s} \equiv \delta p_{\rm de}/\delta\rho_{\rm de} > 0$. The variables of phenomenological approach are connected with scalar field Lagrangian by known relations:

$$\rho_{\rm de} = 2X\mathcal{L}_{,X} - \mathcal{L}, \quad p_{\rm de} = \mathcal{L}, \quad w_{\rm de} = \frac{\mathcal{L}}{2X\mathcal{L}_{,X} - \mathcal{L}}, \quad c^2_{\rm s} = \frac{\mathcal{L}_{,X}}{2X\mathcal{L}_{,XX} + \mathcal{L}_{,X}}, \quad (1)$$

where $\mathcal{L}_{,X} \equiv \partial\mathcal{L}/\partial X$. The phenomenological approach is convenient for practical calculations and putting the observational constraints on model parameters, however gives very little information about the physical nature of dark energy. On the other hand, the scalar field approach is well suited for study of physics of dark energy, but is not as usable in practice as the former one. So it is often useful to combine both methods of modeling of dark energy and use in numerical calculations the phenomenological perfect fluid, while study the physical features of scalar fields reconstructed to mimic the behavior of this perfect fluid. For example, assuming that $c^2_{\rm s} = {\rm const}$ we obtain from (1) the general form of the Lagrangian:

$$\mathcal{L} = VX^\alpha - U,\ U = \frac{c^2_{\rm s} - w_{\rm de}}{1 + c^2_{\rm s}}\rho_{\rm de},\ V = V_0(w_{\rm de} - c^2_{\rm s})\rho_{\rm de},\ X = \left[\frac{1}{V_0}\frac{c^2_{\rm s}}{1 + c^2_{\rm s}}\frac{1 + w_{\rm de}}{w_{\rm de} - c^2_{\rm s}}\right]^{\frac{1}{\alpha}}, \quad (2)$$

where $\alpha \equiv (1+c^2_{\rm s})/(2c^2_{\rm s})$ and V_0 is an arbitrary integration constant. We will analyze here the properties of scalar field dark energy with such Lagrangian at non-stationary cosmological background as well as in stationary spacetime of galaxies and spherical static objects. The spacetime metric we present in the form

$$ds^2 = e^{\nu(t,r)}d\tau^2 - e^{\lambda(t,r)}dr^2 - r^2e^{\mu(t,r)}\left(d\theta^2 + \sin^2\theta d\varphi^2\right), \quad (3)$$

where $e^{\lambda(t,r)} = e^{\mu(t,r)} = a^2(t)$ and $\nu(t,r) = 0$ for cosmological background ($a(t)$ is scale factor), $\nu(t,r) = \lambda(t,r) = \mu(t,r) = 0$ for static Minkowski world and $e^{\nu(r)} = e^{-\lambda(r)} = 1 - r_{\rm g}/r$ and $\mu = 0$ for vicinity of spherical static object with mass M ($r_{\rm g} \equiv 2GM/c^2$ is gravitational radius).

The dependence of dark energy density on time or scale factor a is obtained by integration of the continuity equation $T^i_{0;i}=0$ in the world with metric (3).

So, for non-stationary homogeneous isotropic FRW world the density has the general form for any dependence of EoS parameter $w_{\rm de}$ on scale factor: $\rho_{\rm de}=\rho^{(0)}_{\rm de}a^{-3(1+\tilde{w}_{\rm de})}$ with $\tilde{w}_{\rm de}=(\ln a)^{-1}\int_1^a w_{\rm de}(a)d\ln a$. To specify $w_{\rm de}(a)$ we assume $c^2_{\rm a}\equiv\dot{p}_{\rm de}/\dot{\rho}_{\rm de}=$ const (overdot denotes derivative w.r.t. time τ) which gives the analytical dependences of $w_{\rm de}$ and $\rho_{\rm de}$ on a (Novosyadlyj et al., 2012, 2013):

$$w_{\rm de}=\frac{(1+c^2_{\rm a})(1+w_0)}{1+w_0-(w_0-c^2_{\rm a})a^{3(1+c^2_{\rm a})}}-1,\quad \rho_{\rm de}=\rho^{(0)}_{\rm de}\frac{(1+w_0)a^{-3(1+c^2_{\rm a})}+c^2_{\rm a}-w_0}{1+c^2_{\rm a}} \quad (4)$$

where w_0 is the EoS parameter at the current epoch, $a=1$. For such scalar field its phenomenological density $\rho_{\rm de}$ and pressure $p_{\rm de}$ are analytical functions of a for any values of the constants $c^2_{\rm a}$ and w_0 defining the type and the dynamics of scalar field. Both have the clear physical meaning: w_0 is the EoS parameter $w_{\rm de}$ at current epoch, $c^2_{\rm a}$ is asymptotic value of the EoS parameter $w_{\rm de}$ at early times ($a\to 0$) for $c^2_{\rm a}>-1$ and in far future ($a\to\infty$) for $c^2_{\rm a}<-1$. The asymptotic value of $w_{\rm de}$ in the opposite time direction is -1 in both cases. The examples of evolution tracks of EoS parameter $w_{\rm de}$ for different values of w_0 and $c^2_{\rm a}$ are presented in Fig. 1. (The energy density $\rho_{\rm de}$ and pressure $p_{\rm de}$ are smooth monotonic functions of a for all relations between $c^2_{\rm a}$ and w_0, while $w_{\rm de}$ has a discontinuity of the second kind in the case $w_0<c^2_{\rm a}<-1$ and $-1<c^2_{\rm a}<w_0<0$ when the scalar field energy density passes through zero). So, the Lagrangian of such scalar field model of dark energy can be reconstructed accurately up to a constant V_0 if parameters $\Omega_{\rm de}$, w_0, $c^2_{\rm a}$ and $c^2_{\rm s}$ are given or determined using observational data.

For stationary Minkowski or Schwarzschild world and the scalar field dark energy with $p_{\rm de}(r)/\rho_{\rm de}(r)=w_{\rm de}(r)<0$ and $c^2_{\rm s}=$ const >0 one can obtain (Novosyadlyj et al., 2014a):

$$w_{\rm de}=c^2_{\rm s}-(c^2_{\rm s}-\bar{w}_{\rm de})\bar{\rho}_{\rm de}/\rho_{\rm de}(r), \quad (5)$$

where $\bar{\rho}_{\rm de}$ and $\bar{w}_{\rm de}$ are background values of density and EoS parameters at galaxy background. As it follows from eq. (2) the kinetic term and potential are as follows:

$$X=\left[\pm c^2_{\rm s}\rho_{\rm de}\mp c^2_{\rm s}(c^2_{\rm s}-\bar{w}_{\rm de})\frac{\bar{\rho}_{\rm de}}{1+c^2_{\rm s}}\right]^{\frac{1}{\alpha}},\quad U=\frac{1}{2}\left[(1-c^2_{\rm s})\rho_{\rm de}(r)+(c^2_{\rm s}-\bar{w}_{\rm de})\bar{\rho}_{\rm de}\right].$$

The sign "+" is for quintessential scalar field and "-" for phantom one. When $c^2_{\rm s}=1$ the Lagrangian (2) becomes canonical one: $\mathcal{L}=\pm X-U$.

3 Accelerated expansion of the Universe and $d_{\rm L-z}$ and $d_{\rm A-z}$ cosmological tests

We consider a multicomponent model of the Universe filled by matter (cold dark matter and baryons) with density $\Omega_{\rm m}$, relativistic particles (thermal electromagnetic radiation and massless neutrino) with density $\Omega_{\rm r}$ and a scalar field as described above. The background Universe is assumed to be spatially flat, homogeneous and isotropic with FRW metric. The dynamics of the expansion of the Universe can be deduced from the Einstein equations

$$R_{ij}-\frac{1}{2}g_{ij}R=8\pi G\left(T^{(\rm m)}_{ij}+T^{(\rm r)}_{ij}+T^{(\rm de)}_{ij}\right), \quad (6)$$

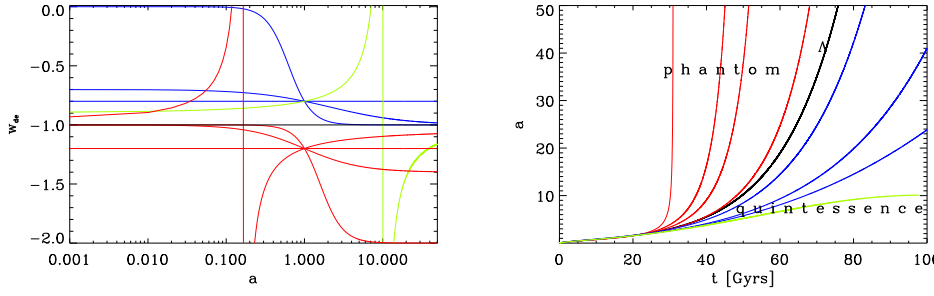

Fig. 1: Left: $w_{\rm de}(a)$ in the expansion Universe for different values of w_0 and $c_{\rm a}^2$. Right: $a(t)$ for cosmological models with scalar field dark energy models and $w_{\rm de}(a)$ from the left panel. ($H = 70$ km s-1 Mpc-1, $\Omega_{\rm m} = 0.3$, $\Omega_{\rm de} = 0.7$ and different sets of values (w_0, $c_{\rm a}^2$): red lines – (-1.2, -2.0), (-1.2, -1.4), (-1.2, -1.2), (-1.2, -1.03), black line – (-1.0, -1.0), blue lines – (-0.8, -0.0), (-0.8, -0.7), (-0.8, -0.8) and green line – (-0.8, -0.9).

where R_{ij} is the Ricci tensor and $T_{ij}^{\rm (m)}$, $T_{ij}^{\rm (r)}$, $T_{ij}^{\rm (de)}$ are the energy-momentum tensors of non-relativistic matter (m), relativistic matter (r), and dark energy (de) respectively. Assuming that the interaction between these components is only gravitational, each of them satisfies the differential energy-momentum conservation law separately: $T^{i\,\rm (N)}_{j;i} = 0$. Einstein's equations together with conservation law equations lead to the Friedmann equations, which describe the rate and acceleration of expansion of the Universe:

$$H = H_0\sqrt{\Omega_{\rm r}/a^4 + \Omega_{\rm m}/a^3 + \Omega_{\rm de}f(a)}, \quad q = \frac{1}{2}\frac{2\Omega_{\rm r} + \Omega_{\rm m}a + (1+3w_{\rm de})\Omega_{\rm de}a^4 f(a)}{\Omega_{\rm r} + \Omega_{\rm m}a + \Omega_{\rm de}a^4 f(a)}, \tag{7}$$

where $f(a) = \rho_{\rm de}(a)/\rho_{\rm de}(1)$. Here $H \equiv \dot{a}/a$ is the Hubble parameter (expansion rate), $q \equiv -a\ddot{a}/\dot{a}^2$ is the deceleration parameter. Eqs. (7) completely describe the dynamics of expansion of the homogeneous and isotropic Universe. In the past it was dominated by radiation and matter, now and in the distant future it is dominated by the scalar field dark energy. The integration of the first Friedmann equation (7) gives us the dependence $a(t)$ shown in the right panel of Fig. 1 for scalar field dark energy with different values of w_0 and $c_{\rm a}^2$. The positive cosmological constant will lead to the exponential expansion $a \propto exp(H\tau)$ in far future (dark line marked by Λ) which is called the late inflation or late de Sitter expansion. The quintessence scalar field dark energy will lead to power-law quasi de Sitter expansion (blue lines). The models with $-1 < c_{\rm s}^2 < w_0 < -1/3$ will cause the turn around and recollapse (green line) to Big Cranch singularity. Fig. 1 illustrates also that the phantom scalar field dark energy will lead to the super-fast expansion of the Universe (red lines), so, that a-infinity is reached within finite time $t_{\rm BR} - t_0 \approx H_0^{-1}|1 + c_{\rm a}^2|^{-1}\sqrt{(1+c_{\rm a}^2)/(1+w_0)/\Omega_{\rm de}}$, which is called as a Big Rip singularity (Caldwell et al., 2003).

In the FRW spacetime the luminosity distance to the source at redshift z with known luminosity L and measured flux F, defined as $d_{\rm L} \equiv \sqrt{L/4\pi F}$, and the angular diameter distance to the source at redshift z with known linear diameter D and measured angular diameter Θ, defined as $d_{\rm A} \equiv D/\Theta$, in the models with given

$\Omega_{\rm de}$	w_0	$c^2_{\rm a}$	$\Omega_{\rm cdm}$	$\Omega_{\rm b}$	H_0
0.718±0.022	$-1.15^{+0.12}_{-0.16}$	$-1.15^{+0.02}_{-0.46}$	0.238±0.022	0.043±0.004	71.4±0.4

Tab. 1: The best-fit values and 2σ confidence limits (C.L.) for parameters of scalar field dark energy ($\Omega_{\rm de}$, w_0 and $c^2_{\rm a}$), density of cold dark matter ($\Omega_{\rm cdm}$), density of baryons ($\Omega_{\rm b}$) and Hubble constant ($H_0\,{\rm km\,s^{-1}\,Mpc^{-1}}$).

cosmological parameters and dark energy model are as follows:

$$d_{\rm L} = (1+z)\int_0^z \frac{dz'}{H(z')}, \quad d_{\rm A} = \frac{1}{1+z}\int_0^z \frac{dz'}{H(z')}. \tag{8}$$

The relation $d_{\rm L} - z$ for "standard candles" and $d_{\rm A} - z$ for "standard meters" are well known cosmological tests for realizations of which a lot efforts of two generations of cosmologists and astrophysicists have been devoted. The first successful realization of $d_{\rm L} - z$ for type Ia Supernovae (SNe Ia) have been done Perlmutter et al. (1998); Riess et al. (1998); Schmidt et al. (1998), which was the first observational evidence for dark energy existence. Since then both cosmological tests have been realized for different redshifts, classes of objects and ranges of electromagnetic radiation. Dozens of independent measurements supported this discovery and constrained the parameters of dark energy (see the above cited reviews) $\Omega_{\rm de}$ and $w_{\rm de}$. For constraining $c^2_{\rm s}$, the density perturbations of dark energy must be taken into account in the computations of large scale structure formation. Since the amplitudes of scalar field dark energy perturbations are essentially lower than dark matter ones at all scales and all epochs the effect is too small to constraining $c^2_{\rm s}$ by current observational data (Novosyadlyj et al., 2012, 2013; Sergijenko & Novosyadlyj, 2015).

In the recent papers to determine the best-fit values and confidence ranges of cosmological parameters and parameters of dark energy, we have used the data on angular power spectra of cosmic microwave background temperature fluctuations (WMAP9 and Planck) (Bennett et al., 2013; Planck Collaboration et al., 2016), Hubble constant measurement (HST) (Riess et al., 2011), baryon acoustic oscillations (BAO) (Beutler et al., 2011; Padmanabhan et al., 2012; Anderson et al., 2012), and SNe Ia luminosity distances (SNLS3 and Union2.1 compilation) (Conley et al., 2011; Suzuki et al., 2012). We use a Markov Chain Monte Carlo routine CosmoMC (Lewis & Bridle, 2002) to map out the likelihood in the multi-dimensional parameter space. Each run has 8 chains converged to $R-1 < 0.01$. The most reliable determination of cosmological and dynamical dark energy parameters are obtained from the Planck+HST+BAO+SNLS3 dataset. The best-fit values and 2σ confidence limits obtained for parameters of scalar field dark energy are presented in the Tab. 1 (for other cosmological parameters see Novosyadlyj et al., 2013). Here $c^2_{\rm s} = 1$ and is fixed since this data set does not determine the effective sound speed (Sergijenko & Novosyadlyj, 2015). This results are in agreement with other determinations (Xia et al., 2013; Rest et al., 2014; Cheng & Huang, 2014; Shafer & Huterer, 2014).

4 Dark energy in the halos and voids

To analyse the behavior of dynamical dark energy in the forming halo and voids the evolution of spherical density and velocity perturbations in three component medium – dark matter, dark energy and radiation, – should be considered from the linear

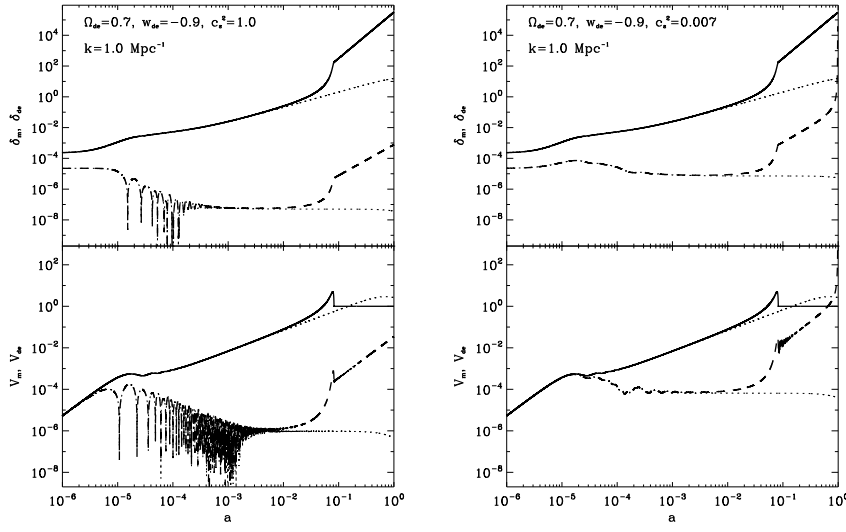

Fig. 2: Evolution of density perturbations of matter $\tilde{\delta}_{\rm m}$ and dark energy $\tilde{\delta}_{\rm de}$, and velocity perturbations of matter $V_{\rm m}$ and dark energy $V_{\rm de}$ in units of Hubble one at the central part of spherical halos. Solid lines corresponds to matter, dashed lines to dark energy and dotted lines show the prediction of the linear theory. (From Novosyadlyj et al., 2016)

superhorizon stage at the radiation dominated epoch to the nonlinear subhorizon one at current epoch. For this purpose, a semi-analytical model based on the integration of the system of partial differential equations describing the evolution of perturbation evolution. Numerical solutions for density and velocity perturbations of dark matter and dark energy allowed us to assess the influence of the latter on the development of elements of the large-scale structure of the Universe. Such approach is described in details in our papers (Novosyadlyj et al., 2016, 2017; Novosyadlyj & Tsizh, 2017).

Up to now it is established that the dynamics of quintessential dark energy in the center of halo or void of dark matter strongly depends on the value of effective sound speed. Fig. 2 illustrates the formation of dark matter halo (solid line) and dynamics of dark energy (dashed line) in the terms of density and velocity peturbations in the reference system which is comoving to the cosmological background. When $c_{\rm s} \sim 1$ the dark energy (type of classical scalar field) is only slightly perturbed and its density is practically the same as the density on the cosmological background (Fig. 2, left). Dark energy with a small value of effective sound speed ($c_{\rm s} \leq 0.1$) is an important dynamic component of the halo: it is capable of accreting into formed halo of dark matter and affecting the value of their finite parameters (Fig. 2, right) (Novosyadlyj et al., 2016). After virialization of the dark matter halo (in Fig. 2 it is at $a_{\rm vir} = 0.083$ ($z_{\rm vir} = 11$)) the matter density $\rho_{\rm m}^{\rm vir} = {\rm const}$, the matter density perturbation $\delta_{\rm m}^{\rm vir} \sim a^3$, since $\delta_{\rm m} \equiv \rho_{\rm m}/\bar{\rho}_{\rm m} - 1$, and peculiar velocity $v_{\rm m}$ equals to Hubble one with opposite sign, or $V_{\rm m}^{\rm vir} \equiv v_{\rm m}/Hr = -1$. On the base of studing of formation of single spherical halos in three component Universe Novosyadlyj et al. (2016) concluded that physical and statistical properties of the most massive earliest virialized structures should discriminate the dark energy with $c_{\rm s} \sim 1$ and $c_{\rm s} \sim 0$. They are now under intensive observational and numerical simulation investigations

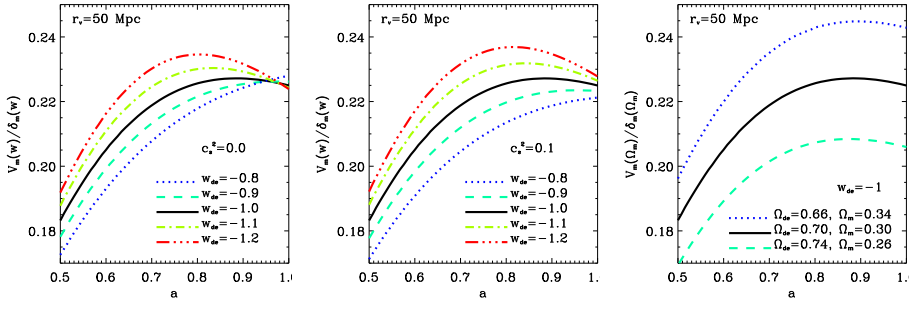

Fig. 3: The ratio $V_{\rm m}/|\delta_{\rm m}|$ for dynamical dark energy models with different values of EoS parameter $w_{\rm de}$, effective sound speed $c_{\rm s}$ and density parameter $\Omega_{\rm de}$ in the cosmological models with zero curvature. (From Novosyadlyj & Tsizh, 2017)

and soon will shed more light on the nature of dark energy.

The giant voids in the large scale structure of the Universe can be useful for determination of dark energy parameters too. Really, the ratio of dark energy density to matter one (dark matter plus baryons),

$$\frac{\rho_{\rm de}^{\rm void}}{\rho_{\rm m}^{\rm void}} = \frac{1+\delta_{\rm de}^{\rm void}}{1+\delta_{\rm m}^{\rm void}}\frac{\Omega_{\rm de}}{\Omega_{\rm m}}, \tag{9}$$

is largest in the voids, since there $-1 < \delta_{\rm m}^{\rm void} < 0$, $|\delta_{\rm m}^{\rm void}| \gg |\delta_{\rm de}^{\rm void}|$. For real voids with $\delta_{\rm m}^{\rm void} \approx -(0.8-0.9)$ in the cosmology with $\Omega_{\rm m} \approx 0.3$ and $\Omega_{\rm de} \approx 0.7$ the ratio is $\approx 12-23$, while at the cosmological background it is 2.3.

The formation of giant voids from the initial adiabatic cosmological perturbations of spacetime metric, density and velocity of matter in cosmological model with dynamical dark energy have been analysed by Novosyadlyj et al. (2017); Novosyadlyj & Tsizh (2017) (see also citations therein). It was shown that the negative density perturbations with the initial radius of about 50 Mpc in comoving to the cosmological background reference system and the amplitude corresponding to the r.m.s. temperature fluctuations of the cosmic microwave background lead to the formation of voids with the matter density contrast up to -0.9, maximal peculiar velocity about 400 km/s and the radius close to the initial one. An important feature of voids formation from the analyzed initial amplitudes and profiles is establishing the surrounding matter overdensity shell. The evolution of dark energy density and velocity perturbations strongly depends on the values of $w_{\rm de}$ and $c_{\rm s}$. It was shown also that the ratio of the peculiar velocity of matter in units of the Hubble flow to the matter density contrast in the central part of a void is sensitive to the values of dark energy parameters that is shown in Fig. 3. Hence the observational data on mass density and peculiar velocities of galaxies in the voids can be used for determination of parameters of dark energy.

5 Scalar field dark energy in the galaxies

We suppose that the spacetime in stationary galaxies and clusters is the Minkowski one and the EoS parameter $w_{\rm de}$ varies with variation of local density of scalar field $\rho_{\rm de}$ according to eq. (5). For the estimation of the value of background density

of dark energy $\bar{\rho}_{\rm de}$ and matter $\bar{\rho}_{\rm m}$ in the galaxies one can use the halo model of galaxies and clusters formation (Smith et al., 2003; Kulinich et al., 2013). According to this model, the average density of matter after virialization and establishing of the dynamical equilibrium is $\rho_{\rm m}^{\rm vir} = \Delta_{\rm vc}\rho_{\rm cr}(z_{\rm col})$, where $\Delta_{\rm vc} \approx 100$ in current epoch, ≈ 150 at $z = 1$ and ≈ 180 at $z > 10$, and critical density is taken for the moment of collapse of the central part of the uniform dust-like halo. For further estimation we assume that the redshift of the collapse $z_{\rm col}$ is 20 for typical galaxy and 1 for typical cluster of galaxies. The simple estimations (see for details Novosyadlyj et al., 2014b) give the average matter density in typical massive galaxy and rich cluster of galaxies $\rho_{\rm m}^{\rm gal} \approx 5 \times 10^{-24}\,{\rm g\,cm^{-3}}$, $\rho_{\rm m}^{\rm cl} \approx 5 \times 10^{-27}\,{\rm g\,cm^{-3}}$.

Scalar field as dark energy, which almost uniformly fills the entire Universe, practically does not participate in the virialization of the dark matter, but it feels the changes of the gravitational potential of the halo in the time and space. After the halo (galaxy or cluster of galaxies) has been separated from the expansion of the Universe, which happens at the moment $z_{\rm ta}$ ($t_{\rm ta} = t_{\rm col}/2$ in Einstein-de Sitter model), the dynamics of dark energy changes according to the dynamics of local world. When halo after virialization is stabilized, the static world in its volume can be considered as Minkowski world (we ignore here local inhomogeneities and curvature of spacetime). For estimation we assume that the dynamics of dark energy in galaxies and clusters stabilizes at their $z_{\rm col}$ and from this moment its density does not change. As $\rho_{\rm de}(z) = \Omega_{\rm de}\rho_{\rm cr}^{(0)}(1+z)^{3(1+w_{\rm de})}$, for quintessential scalar field with $w_{\rm de} = -0.9$ for galaxy and cluster of galaxies we get $\rho_{\rm de}^{\rm gal} \approx 2 \times 10^{-29}\,{\rm g\,cm^{-3}}$, $\rho_{\rm de}^{\rm cl} \approx 8 \times 10^{-30}\,{\rm g\,cm^{-3}}$, and for phantom field respectively $\rho_{\rm de}^{\rm gal} \approx 2.5 \times 10^{-30}\,{\rm g\,cm^{-3}}$, $\rho_{\rm de}^{\rm cl} \approx 5.2 \times 10^{-30}\,{\rm g\,cm^{-3}}$. So, in the galaxies and clusters $\rho_{\rm de} \ll \rho_{\rm m}$.

Another important question connected with properties of dark energy in a stationary world is addressed to its gravitational instability. Our analysis (Novosyadlyj et al., 2014b) showed that scalar field dark energy with Lagrangian (2) and EoS (5) is stable and can only oscillate with constant amplitude on scales smaller than the Jeans scale $\lambda_{\rm J} \approx 2660(1+3c_{\rm s}^2)^{-1/2}(1+w_{\rm de})^{-1/2}(6.4\times10^{-30}/\rho_{\rm de})^{1/2}$ Mpc, which for realistic values of $\rho_{\rm de}$ (in g cm^{-3}) is much larger than the scales of observable structures interesting for astrophysics. Phantom dark energy has no Jeans scale – the perturbations on all scales can only oscillate with constant amplitude.

In the two-component medium the amplitudes of the dark matter density perturbations are much larger than the dark energy ones and almost completely determine the gravitational potential of perturbations on given scale (Novosyadlyj et al., 2014b). Dark energy can monotonically flow into gravitational potential wells of positive matter density perturbations ($\delta_{\rm m} > 0$) oscillating with significantly lower constant amplitude and forming dark energy overdensity ($\delta_{\rm de} > 0$) in the case of quintessential dark energy ($-1 < w_{\rm de} < -1/3$) and dark energy underdensity ($\delta_{\rm de} < 0$) in the case of phantom one ($w_{\rm de} < -1$). We should note, however, that the amplitudes of perturbations of dark energy at all galaxy and cluster scales are negligibly small in comparison with amplitudes of perturbations of dark matter ($\delta_{\rm de} \ll \delta_{\rm m}$, $V_{\rm de} \ll V_{\rm m}$). Only in the models of dark energy with $c_{\rm s} \to 0$ the velocity perturbations of dark energy are close to velocity perturbations of matter: $V_{\rm de} \to V_{\rm m}$, while $\delta_{\rm de} \to (1+w_{\rm de})\delta_{\rm m}$. If $c_{\rm s} \geq 0.1$, then $V_{\rm de} \leq 10^{-3}V_{\rm m}$ on the largest scales of galaxies and $V_{\rm de} \leq 10^{-2}V_{\rm m}$ on the largest scales of clusters of galaxies. So, the amplitudes of perturbations of dark energy may be larger in the dynamical models of dark energy with small value of speed of sound and may leave traces in

the structure on scales of galaxies and clusters of galaxies.

6 Scalar field dark energy in the vicinities of stars and black holes

Static distribution. One more important question regarding dynamical dark energy is connected with its behavior in the strong gravitational fields of massive compact objects in galaxies, e.g. globular clusters, stars or black holes. It can be formulated as follows: whether or not some possibility exists for dark energy to be agglomerated in large enough amounts to have some manifestation in spite of its negligible mean density in galaxies? To get an answer we have analyzed (Novosyadlyj et al., 2014b) the dynamics of scalar field with Lagrangian (2) and EoS (5) in the gravitational fields of non-rotational stars and black holes, in the vicinities of which the spacetime metric is the Schwarzschild one.

The first important conclusion of such analysis is existence of a static solution for dark energy in the gravitational fields of spherical static objects. The equation expressing the static condition is the only nontrivial energy-momentum conservation law equation $T^k_{1\,;k} = 0$:

$$\frac{dp_{\rm de}}{dr} + \frac{1}{2}(\rho_{\rm de} + p_{\rm de})\frac{d\nu}{dr} = 0, \tag{10}$$

where $p_{\rm de}$ and $\rho_{\rm de}$ are unknown functions of r, $\nu(r)$ is metric function for Schwarzschild spacetime (see eq. (3) and text after it). For a scalar field with Lagrangian (2) and EoS (5) the equation (10) is integrated and gives the dependence of the density of dark energy on the radial coordinate,

$$\rho_{\rm de}(r) = \bar{\rho}_{\rm de}\left(\frac{c_{\rm s}^2 - \bar{w}_{\rm de}}{1+c_{\rm s}^2} + \frac{1+\bar{w}_{\rm de}}{1+c_{\rm s}^2}\left[e^{\nu(r)}\right]^{-\frac{1+c_{\rm s}^2}{2c_{\rm s}^2}}\right), \tag{11}$$

where $e^{\nu(r)} = 1 - r_{\rm g}/r$ outside the spherical object and $e^{\nu(r)} = (1-\alpha)^{3/2}/(1-\alpha r^2/R^2)^{1/2}$ inside it, where $\alpha \equiv r_{\rm g}/R$ and R is radius of object. Such dependences for quintessential and phantom scalar field dark energy with different values of effective sound speed are shown in the left panel of Fig. 4. So, the density of dark energy deviates gradually from $\bar{\rho}_{\rm de}$ when we approach the spherical static object. The character (increasing or decreasing) and rate of change depend on type of dark energy (quintessence or phantom), parameters of the background dark energy, $c_{\rm s}^2$ and $\bar{w}_{\rm de}$, as well as on the gravitational radius of the central body. It should be noted that for $c_{\rm s}^2 \to 0$ the solution (11) loses its meaning. This means that static solutions do not exist for dark energy with $c_{\rm s}^2 = 0$: it can only inflow (accrete) on a spherical static object or outflow from its neighborhood. One can see that the density of quintessential dark energy grows up with approaching the spherical static object and reach the maximum value in the center, which for objects with $\alpha \ll 1$ is $\rho_{\rm de}(0) \approx \bar{\rho}_{\rm de}\left(1 + \alpha(1+\bar{w}_{\rm de})/c_{\rm s}^2\right)$. The estimations of magnitude of $(\rho_{\rm de}(0) - \bar{\rho}_{\rm de})/\bar{\rho}_{\rm de}$ for planets, stars, galaxies and clusters of galaxies, show that it is very small $\sim 10^{-7} - 10^{-10}$ if $c_{\rm s}^2 \sim 1$. Taking into account the smallness of the mean dark energy density in the galaxies and clusters of galaxies we can conclude that the influence of dark energy with $c_{\rm s}^2 \sim 1$ on the structure of these objects or on the dynamics of the other bodies in their gravitational field is negligible. In contrast, the dark energy with $c_{\rm s}^2 \sim 0$ can agglomerate in the vicinity of compact spherical object and affect their dynamics or orbits of their satellites and so on. Thus, for such dark energy we

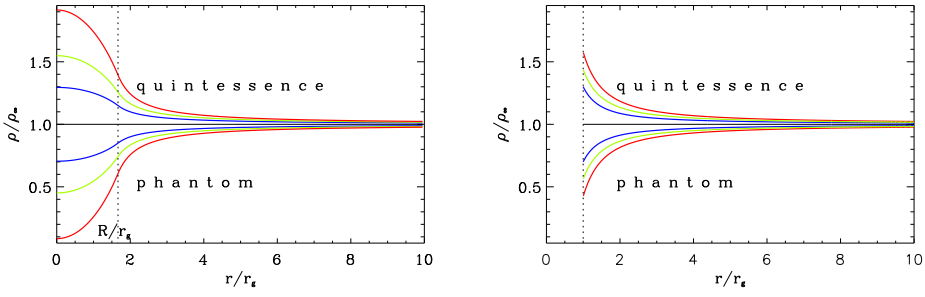

Fig. 4: The dependence of density of dark energy on distance from the center of central body for quintessence ($w_\infty = -0.8$) and phantom ($w_\infty = -1.2$) scalar field with effective sound speed c_s^2 =1 (blue lines), 2/3 (green lines), 1/2 (red lines) from bottom to top for quintessence dark energy and from top to bottom for phantom dark energy. Left panel: homogeneous spherical object with $R/r_g = 5/3$, distribution for condition of static equilibrium; right panel: black hole, distribution for stationary accretion condition.

can expect observational manifestations on astrophysics scales. Their absence can give us a low limit for the value of c_s^2. Moreover, the scalar field dark energy with Lagrangian (2) and EoS parameter (5) transforms into scalar field dark matter with satisfied energy conditions $\rho_{de}(r) + p_{de}(r) > 0$ and $\rho_{de}(r) + 3p_{de}(r) > 0$ in the dark energy dense regions with $\rho_{de}(r) \geq 3\bar{\rho}_{de}(c_s^2 - \bar{w}_{de})/(1 + 3c_s^2)$.

Fig. 4 shows also that the density of phantom dark energy in the potential wells of the spherical static objects is lower than the background density and tends to zero when the size of the object approaches the value of the gravitational radius. This may mean that phantom dark energy avoids neutron stars and black holes, $\rho_{de} \to 0$.

Stationary accretion onto black hole. Eq. (11) shows also that a static solution does not exist for black holes, since the singularity is for ρ_{de} at $r = r_g$. Therefore the dynamical dark energy can inflow or outflow from vicinities of black holes. In the assumptions of test dark matter, which does not change the spacetime metric, and stationary dark energy flow such problems were solved by different authors for different physical scenarios (see recent review Babichev et al., 2013, and references therein).

The assumption of stationary accretion of dark energy means that it inflow in black hole vicinity but its density and flow velocity depend on radial distance and do not depend on time. In (Novosyadlyj et al., 2014a) we have analyzed accretion of scalar field dark energy with Lagrangian (2) and EoS parameter (5) onto black hole and have obtained the analytical solutions of equations $T^i_{k\,;i} = 0$ for density and velocity of dark energy as test component in the Schwarzschild field. The analytical radial dependence of density $\rho_{de}(r)$ and 3-velocity $v_{de}(r)$ of dark energy is obtained for some special values of c_s^2. In the right panel of Fig. 4 the dependences of $\rho_{de}(r)$ for quintessence ($w_\infty = -0.8$) and phantom ($w_\infty = -1.2$) scalar field with effective sound speed c_s^2 =1, 2/3 and 1/2 are presented for the case of stationary accretion onto black hole. They are quite similar to static distributions of ρ_{de} in the vicinity of neutron star like object with $r_g/R = 0.6$, which is shown in the left panel of this figure. So, above speculations about stationary distributions of dark energy in the vicinities of spherical static objects can be repeated for distributions in the case of

stationary accretion of test scalar field dark energy onto black hole.

The important characteristic of accretion of dark energy onto black hole is the rate of change of the inflow mass of dark energy, which in our case is (Novosyadlyj et al., 2014a):

$$\dot{m} = \pi \frac{(1+3c_{\rm s}^2)^{\frac{1+3c_{\rm s}^2}{2c_{\rm s}^2}}}{4c_{\rm s}^3}(1+w_\infty)\rho_\infty R_{\rm g}^2. \qquad (12)$$

It shows that the quintessential scalar field dark energy inflows ($\dot{m} > 0$) onto the black hole, while the phantom one outflows ($\dot{m} < 0$). This can be easy understood in the framework of Newtonian dynamics if we take into account that the inertial mass of dark energy in the element of volume is $\propto (\rho_{\rm de} + p_{\rm de})$ and is positive for the quintessential dark energy and negative for the phantom one. Thus, the quintessential scalar field is pulled into the gravitational potential wells of static objects while the phantom field is pushed out of them. The direction of movement depends on the resultant force, which is the vector sum of the gravitational pulling/pushing forces and the pressure gradient. To evaluate the direction of resultant force one can calculate the right hand side of eq. (10) using eq. (5) and analytical solutions for $\rho_{\rm de}(r)$ for stationary accretion onto a black hole, presented in (Novosyadlyj et al., 2014a). The total force acting on the element of quintessential dark energy is directed to the center, while for the phantom one it is directed from the center. This also explains the avoidance of phantom dark energy in the potential wells of astrophysical objects.

Eq. (12) also shows that the mass of quintessential dark energy accreted onto black hole is large for the model with a lower value of the effective sound speed. So, for some low value of $c_{\rm s}^2$ the assumption about the test scalar field becomes wrong and the backreaction of inflow matter on the spacetime metric must be taken into account. Such models are most interesting since they would have observational manifestations which can be used for unveiling the nature of dark energy.

References

Amendola, L., Tsujikawa, S., Dark Energy: Theory and Observations (2010)

Anderson, L., et al., *MNRAS* **427**, 3435 (2012)

Babichev, E. O., Dokuchaev, V. I., Eroshenko, Y. N., *Physics Uspekhi* **56**, 12, 1155-1175 (2013)

Bennett, C. L., et al., *ApJS* **208**, 20 (2013)

Beutler, F., et al., *MNRAS* **416**, 3017 (2011)

Caldwell, R. R., Kamionkowski, M., Weinberg, N. N., *Physical Review Letters* **91**, 7, 071301 (2003)

Cheng, C., Huang, Q.-G., *Phys. Rev. D* **89**, 4, 043003 (2014)

Conley, A., et al., *ApJS* **192**, 1 (2011)

Ellis, G., Nicolai, H., Durrer, R., Maartens, R., *General Relativity and Gravitation* **40**, 219 (2008)

Huterer, D., Turner, M. S., *Phys. Rev. D* **60**, 8, 081301 (1999)

Kulinich, Y., Novosyadlyj, B., Apunevych, S., *Phys. Rev. D* **88**, 10, 103505 (2013)

Lewis, A., Bridle, S., *Phys. Rev. D* **66**, 10, 103511 (2002)

Novosyadlyj, B., Kulinich, Y., Tsizh, M., *Phys. Rev. D* **90**, 6, 063004 (2014a)

Novosyadlyj, B., Pelykh, V., Shtanov, Y., Zhuk, A., *arXiv e-prints* (2015)

Novosyadlyj, B., Sergijenko, O., Durrer, R., Pelykh, V., *Phys. Rev. D* **86**, 8, 083008 (2012)

Novosyadlyj, B., Sergijenko, O., Durrer, R., Pelykh, V., *J. Cosmology Astropart. Phys.* **6**, 042 (2013)

Novosyadlyj, B., Tsizh, M., *arXiv e-prints* arXiv:1703.00364 (2017)

Novosyadlyj, B., Tsizh, M., Kulinich, Y., *Kinematics and Physics of Celestial Bodies* **30**, 53 (2014b)

Novosyadlyj, B., Tsizh, M., Kulinich, Y., *General Relativity and Gravitation* **48**, 30 (2016)

Novosyadlyj, B., Tsizh, M., Kulinich, Y., *MNRAS* **465**, 482 (2017)

Padmanabhan, N., et al., *MNRAS* **427**, 2132 (2012)

Perlmutter, S., et al., *Nature* **391**, 51 (1998)

Planck Collaboration, et al., *A&A* **594**, A13 (2016)

Rest, A., et al., *ApJ* **795**, 44 (2014)

Riess, A. G., et al., *AJ* **116**, 1009 (1998)

Riess, A. G., et al., *ApJ* **730**, 119 (2011)

Ruiz-Lapuente, P., Dark Energy: Observational and Theoretical Approaches (2010)

Schmidt, B. P., et al., *ApJ* **507**, 46 (1998)

Sergijenko, O., Novosyadlyj, B., *Phys. Rev. D* **91**, 8, 083007 (2015)

Shafer, D. L., Huterer, D., *Phys. Rev. D* **89**, 6, 063510 (2014)

Smith, R. E., et al., *MNRAS* **341**, 1311 (2003)

Suzuki, N., et al., *ApJ* **746**, 85 (2012)

Wolschin, G. (ed.), Lectures on Cosmology Accelerated Expansion of the Universe, *Lecture Notes in Physics, Berlin Springer Verlag*, volume 800 (2010)

Xia, J.-Q., Li, H., Zhang, X., *Phys. Rev. D* **88**, 6, 063501 (2013)